

TR/08/82

July 1982

PARTIAL DIFFERENTIAL EQUATIONS  
IN MEDICAL BIOPHYSICS

E.H. Twizell

To appear in *Applied Mathematics Notes* of the  
Canadian Mathematical Society. A shortened  
version will appear in the *Brunel Bulletin*,  
December 1982.



## **PARTIAL DIFFERENTIAL EQUATIONS IN MEDICAL BIOPHYSICS**

**E. H. Twizell**

**Department of Mathematic  
Brunel University  
Uxbridge Middlesex  
England UB8 3PH**

### **0. ABSTRACT**

A number of examples of collaborative research are outlined which show how mathematicians and medical biophysicists have contributed to a wider understanding of some problems in applied physiology.

### **1. INTRODUCTION**

A few decades ago the techniques developed by mathematicians were used only by physicists and engineers. Nowadays, however, researchers in a considerable number of other, widely varying disciplines use mathematics to help solve their problems.

More non-mathematicians have begun to use mathematics *via* mathematical modeling which has received an upsurge in interest. Many universities have introduced courses in mathematical modeling at both undergraduate and graduate levels which have attracted mathematicians and non-mathematicians alike. Simultaneously, students have received training in the programming of digital computers and have thus had the powerful combination of mathematical modelling with computer simulation at their disposal.

The student has been helped by the growth in the number of texts on mathematical and computer modelling, most of which present the reader with case studies after an introduction to the philosophy of mathematical modelling. One such text, by Burghes and Borrie [2], is of

(2)

particular interest to teachers and students both at high school and undergraduate level, and gives a very wide range of interesting applications of mathematics. The number of journals placing emphasis on the use of mathematical modelling and computer simulation has also increased. These journals are directed at all academic disciplines and levels. Interdisciplinary research conferences, at which mathematicians and workers in other disciplines are able to exchange views, are attracting the financial support of research councils and other bodies.

One example, of late, in this fertilization of ideas, is the boom in collaboration between researchers in mathematics and computer science on the one hand, with researchers in biology and medicine on the other. The fruits of these partnerships, in such wide fields as applied physiology and bioengineering, are enormously beneficial to mankind.

Mathematical modeling of any aspect of the human body is a tricky process. Many advanced models express the physiological behaviour of the body in the form of a system of differential equations, ordinary or partial, with initial conditions and boundary conditions specified. Often, it is the boundary conditions, which depend on the non-uniform geometry of the body, which give rise to difficulties in solving the differential equations. Indeed, it is frequently too difficult, or impossible, to find the theoretical solution of the system and the mathematician resorts to finding a numerical solution to the problem, using a digital computer to calculate the results.

In the following sections of this paper case studies are outlined, relating to the three types of second order partial differential equation, of three physiological problems modelled recently in the literature. It will be easy for the reader to see how the complicated geometry of the body must be approximated to facilitate the determination of even a numerical solution.

## 2. ELLIPTIC EQUATIONS

One human organ which has an irregular, curved boundary is the *otolith*

(3)

*membrane*. Under the microscope, the otolith membrane is seen to be roughly the shape of a kidney bean with jagged edges. The membrane is a thin layer of gelatine; it is one component of the non-auditory part of the inner ear, and is associated with the stability and equilibrium of the body and stabilizing the eyes during movements of the head. Crystals of calcite (called the *otoconia* and sensitive hairs (called the *stereocilia*) adhere to the otolith. The density of the crystals is much greater than the density of the otolith and in the normal upright position of the head the sensitive hairs protrude vertically upwards.

Disturbance of the head from the normal upright position initiates movement of the otoconia down the slope of the membrane. This movement distorts the elastic membrane, causes shearing forces in the cilia, and cause electrical signals to be sent to the brain. The frequency and amplitude of these signals are related to the magnitude and direction of the displacements of the points of the membrane. The brain's interpretation of these signals initiates responding movements of the head for stabilizing the eyes and restoring balance. Thus, the magnitudes and directions of displacements of points of the membrane for various head movements are of importance in any study of the otolith organs.

Numerical modelling of the otolith membrane makes this possible; such models have been developed by Hudetz [4], Twizell and Curran [16,18] and in the unpublished dissertation of Finlayson [3]. These models assume a membrane with Poisson ratio  $\nu = 0.5$ , Young's modulus  $E = 200000 \text{ dynes cm}^{-2}$  and density  $\rho = 0.903 \text{ gm cm}^{-3}$ .

In developing a mathematical model of a human organ such as the otolith membrane, it is essential that a reasonably close approximation to the irregular boundary be made. The maximum length of a typical membrane is about 0.256 cm and the maximum breadth is about 0.192 cm; the approximate shape of the boundary  $\partial R$  is shown in Figure 1.

(4)

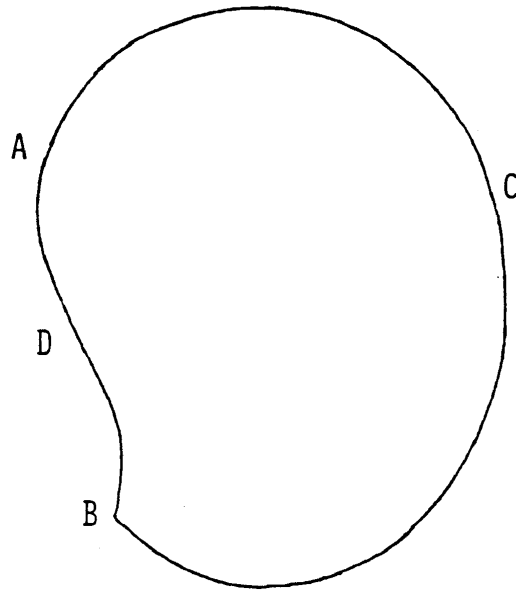


**Figure 1**

The portion ACB is given by the ellipse (Twizell [16])

$$\frac{x^2}{0.009216} + \frac{y^2}{0.016384} = 1$$

and the portion ADB by the polynomial (Finlayson [3])

$$x = -0.084 - 0.5y + 2.1701 y^2 + 54.2535 y^3.$$

The enclosed region  $R$  of the membrane is assumed to lie in the plane  $z=0$  when the head is in its normal upright position, with the  $z$ -axis passing through the point 0.

It was noted in [4] that the components of the gravitational force on the points of the membrane in the  $x$  and  $y$  directions resulting from a rotation of the head through an angle  $\alpha$  about the  $x$ -axis, followed by a rotation through an angle  $\beta$  about the  $y$ -axis, followed by a rotation through an angle  $\gamma$  about the  $z$ -axis, are given by

$$F^{(x)} = \rho g \{ \cos \psi (\sin \alpha \sin \gamma + \cos \alpha \sin \beta \cos \gamma) + \sin \psi (\sin \alpha \cos \gamma - \cos \alpha \sin \beta \sin \gamma) \},$$
$$F^{(y)} = \rho g \{ -\sin \psi (\sin \alpha \sin \gamma + \cos \alpha \sin \beta \cos \gamma) + \cos \psi (\sin \alpha \cos \gamma - \cos \alpha \sin \beta \sin \gamma) \},$$

respectively, where  $\psi$  is the azimuth angle and  $g$  is the acceleration due to gravity.

(5)

The steady-state displacements  $u, v$  in the positive  $x, y$  directions of points of the membrane are governed by the system of elliptic partial differential equations given by

$$\frac{\partial^2 u}{\partial x^2} + \frac{1-\nu}{2} \frac{\partial^2 u}{\partial y^2} + \frac{1+\nu}{2} \frac{\partial^2 v}{\partial x \partial y} + \frac{1-\nu^2}{E} F^{(x)} = 0, \quad (1)$$

$$\frac{\partial^2 v}{\partial y^2} + \frac{1-\nu}{2} \frac{\partial^2 v}{\partial x^2} + \frac{1+\nu}{2} \frac{\partial^2 u}{\partial x \partial y} + \frac{1-\nu^2}{E} F^{(y)} = 0, \quad (2)$$

in  $R$ , together with the Dirichlet boundary conditions

$$u(x, y) = v(x, y) = 0 \quad (3)$$

for all  $(x, y) \in \partial R$ .

Numerical solutions of equations (1), (2) with boundary conditions (3) were obtained using finite element methods in [18], and using finite difference methods in [3], [4], [16] for a number of different rotations of the head.

Changing the value of  $g$  in the expressions for  $F^{(x)}$ ,  $F^{(y)}$  changes the numerical solution of (1), (2) with (3). In this way gravitational conditions in locations other than on the surface of the Earth may be simulated and the resultant displacements of points of the membrane computed in each location for any movement of the head (Twizell [16]).

### 3. HYPERBOLIC EQUATIONS

Replacing the right hand sides of (1), (2) with  $\partial^2 u / \partial t^2$ ,  $\partial^2 v / \partial t^2$  respectively converts the system into the hyperbolic type. Specifying initial values for  $u, v, \partial u / \partial t, \partial v / \partial t$  thus enables the displacements of points of the membrane to be calculated at any time  $t > 0$  following the instantaneous rotations  $(\alpha, \beta, \gamma)$  from the normal upright position of the head (at time  $t = 0$ ). As  $t \rightarrow \infty$ , the computed solutions  $U, V$  of the hyperbolic system converge to the steady state solution of the elliptic system discussed in §2.

(6)

Approximating the space derivatives of the hyperbolic system with finite difference replacements leads to a system of second order ordinary differential equations of the form

$$\frac{d^2 \underline{w}}{dt^2} = A \underline{w} + \underline{b}; \quad \underline{w}(0) = \underline{0}, \quad \frac{d\underline{w}}{dt}(0) = \underline{f}, \quad (4)$$

where the constant matrix  $A$  depends on the space discretization of the membrane and on the finite difference replacements of the space derivatives, and the vector  $\underline{b}$  depends on the applied forces  $F^{(x)}$  and  $F^{(y)}$ ; the elements of the vector  $\underline{w}$  are the computed values  $U, V$  of the displacements of the discrete points of  $R$  at time  $t > 0$ , and  $\underline{f}$  is the vector of initial speeds down the slope of the membrane. The order of the matrix  $A$ , the vectors  $\underline{b}$ ,  $\underline{w}$ ,  $\underline{f}$ , and consequently the system (4), is  $2N$ , where  $N$  is the number of points at which  $R$  is discretized.

It was shown in [3] that the solution  $\underline{w}(t)$  of the initial value problem (4) satisfies the recurrence relation

$$\begin{aligned} \underline{w}(t + \ell) - \{\exp(\ell B) + \exp(-\ell B)\} \underline{w}(t) + \underline{w}(t - \ell) \\ = \{\exp(\ell B) + \exp(-\ell B)\} A^{-1} \underline{b} - 2A^{-1} \underline{b}, \end{aligned} \quad (5)$$

where  $\ell$  is a convenient time step and  $B$  is a matrix such that  $B^2 = A$ . Replacing the matrix functions  $\exp(\ell B)$  and  $\exp(-\ell B)$  with padé approximants ensures that odd powers of  $\ell B$  vanish, so that the matrix  $B$  need not be determined explicitly. The computed solution of (5) will depend for its accuracy in time on the padé approximant chosen and a stability analysis of the resulting algorithm is carried out in the usual way; for a consistent algorithm the (0,1) and (1,0) padé approximants may not be used.

One more occurrence of a second order hyperbolic partial differential equation is in the mathematical modelling of arterial blood pressure. It is often difficult to estimate values of arterial blood pressure in healthy arteries and numerous examples of collaborative research between mathematicians and physiologists have become evident in recent times. In the papers by Stettler *et al* [12a, 12b] for instance, a



(7)

mathematical model is developed for the prediction of the pressure and flow pulses in arteries. The model considers branches, bifurcations and stenoses and the numerical predictions are compared with laboratory findings. The development of the mathematical model by Anliker *et al* [1a, 1b] was undertaken because of the need for a noninvasive method of determining, in advance, possible changes which may occur in the cardiovascular system of astronauts as a result of prolonged exposure to weightlessness. Mathematical models of pressure and flow in arterial stenoses are discussed using finite element methods in Wille [20] and finite difference methods in Wille and Walløe [21]. Calculations using characteristics are carried out by Rumberger and Nerem [8] and are compared with earlier laboratory results. An historical perspective on the development of the mechanics of blood flow is given in the excellent review paper by Skalak *et al* [9] who include a list of 154 references of other review papers, texts and theoretical and practical research papers.

A simple mathematical model of arterial blood pressure in a cylindrical artery of length  $L$ , inner radius  $R$  and thickness  $H$  was discussed by Twizell [17]. Young's modulus for the arterial wall is denoted by  $E$ , Poisson's ratio for the wall by  $\sigma$ , and the density of blood by  $\rho$ . It is assumed that the artery is sufficiently remote from the heart for a sinusoidal formulation to be appropriate and that the heart beats steadily at  $T$  contractions per second.

The arterial blood pressure  $u(x,t)$  at a point  $x$  units along the length of the artery at time  $t$  is known to satisfy the hyperbolic equation

$$c^2 \frac{\partial^2 u}{\partial x^2} = \frac{\partial^2 u}{\partial t^2} \quad ; \quad 0 < x < L, \quad t > 0, \quad (6)$$

where  $c$  denotes the velocity of propagation of a pressure wave and is a function of the elastic and physical properties of the artery and the effects of viscosity; it is given by

$$c^2 = \frac{EH}{2R_\rho(1-\sigma^2)} - \frac{u}{\rho}.$$

(8)

Writing  $c$  in this form makes the model capable of dealing with changes in the velocity of propagation of a pressure wave, and in the arterial pressure itself, due to a number of physiological changes brought about by arteriosclerosis, coagulation or thrombosis. The serious limitations of such a simple model are that important features such as junctions or curves in the artery, reflected pressure waves, and localized changes in the inner radius or thickness of the arterial wall are not considered.

The boundary conditions which the solution of (6) must satisfy are given by

$$u(0, t) = \frac{1}{2} V(1 + \cos 2\pi Tt) \quad , \quad t > 0$$

$$u(L, t) = \frac{1}{2} V(1 + \cos \frac{2\pi TL}{c} \cos 2\pi Tt) \quad , \quad t > 0$$

and the initial conditions are given by

$$u(x, 0) = \frac{1}{2} V(1 + \cos \frac{2\pi Tx}{c}) \quad , \quad 0 \leq x \leq L$$

and

$$\frac{\partial u}{\partial t}(x, 0) = 0,$$

where  $V$  is the pressure at the inlet of the artery.

It is easy to deduce that

$$\frac{\partial u}{\partial x}(x, 0) = -\frac{\pi TV}{c} \sin \frac{2\pi Tx}{c} \quad , \quad 0 \leq x \leq L$$

and the method of characteristics may now be used to find the computed value of  $u$  by first discretizing the initial conditions at a number of points along the length of the artery. The  $x$ -coordinates of the nodes of the characteristic mesh generated are found to be almost coincident with the  $x$ -coordinates of the initial points so that arterial pressure at any point along the artery can be monitored fairly closely.

#### 4. PARABOLIC EQUATIONS

Parabolic equations arise in the flow of heat in the human body and for the environmental temperature range normally encountered by the body, experimental data do exist against which mathematical predictions may be compared. Arguably the most important segment of the body, in so far as heat flow is concerned, is the torso (that part of the body not including the head, neck or limbs), as almost 77% of cardiac output is to this segment which must therefore be maintained at a comfortable temperature.

The most sophisticated mathematical models of heat flow in the human torso consider the torso to consist of four concentric circular layers of different types of tissue, namely core, muscle, fat and skin [6,10, 11,19] or as elliptic cylindrical layers of tissue [19]. The main advantage of assuming an elliptic cross-section is that the geometry of a cross-section of the normal male human torso is approximately an ellipse; the main disadvantage is that the algebraic manipulation involved in the computation of heat flow is much more difficult. In assuming three space dimensions, the model is able to deal with non-uniform longitudinal environmental temperatures; such models also involve increased computational difficulties [19].

The majority of models of heat flow in the human torso are two dimensional and, because the effective thermal conductivity of the core is approximately the same as that of the muscle and the effective thermal conductivity of the fat is approximately the same as that of the skin, have only two concentric layers of tissue. These layers are usually referred to as *core* and *the insulating layer* and their thicknesses are assumed to be in the approximate ratio 7:1.

Other factors governing the regulation of temperature within the torso include the generation of heat by metabolic reactions; convection of heat by flowing blood; heat exchange between large arteries and veins; heat loss due to sweating and shivering; loss of heat at the skin surface due to convection, evaporation and radiation; and environmental conditions. Open and closed loop simulations involving these factors were dealt with fully in the doctoral thesis of Smith [10]. This work

incorporated the control system developed by Stolwijk and Hardy [13,14,15] which was validated experimentally by Konz *et al* [5].

Some of the most important uses of mathematical models of heat flow in the torso have been in the analysis of physiological and bioengineering problems associated with the disparate environments encountered in space flight. Such research has been carried out extensively at the Lyndon B. Johnson Space Center (NASA), Houston, Texas to aid in the design and understanding of the physiological effects of liquid-cooled garments, the study of human thermal stress, and the study of performance under conditions of strenuous exercise in extreme environments (see Kuznetz [6]). The modelling of heat flow in the human torso in an industrial environment has been carried out at the Institute for Systems Design and Optimization, Department of Industrial Engineering, Kansas State University by Fan, Hsu, Hwang, Konz *et al*.

Considering a two-dimensional, time dependent model with a circular cross-section of radius  $a$ , consisting of the two-shell core/insulating layer concept, the temperature  $u = u(r, \theta, t)$  at the point  $(r, \theta)$  at some time  $t > 0$  is known to satisfy the parabolic equation

$$(\rho C)_s \frac{\partial u}{\partial t} = \kappa_s \left\{ \frac{\partial^2 u}{\partial r^2} + \frac{1}{r} \frac{\partial u}{\partial r} + \frac{1}{r^2} \frac{\partial^2 u}{\partial \theta^2} \right\} + q_s(u) + H_{VS}(T_V - u) + [(\dot{m}C)_{CS} + H_{as}][T_a - u]. \quad (7)$$

In (7) the subscript  $s = 1, 2$  refers to the core, insulating layer, respectively;  $\rho$ ,  $C$ ,  $\kappa$ ,  $q$  denote density, heat capacity, thermal conductivity, heat generation rate, respectively;  $(\dot{m}C)_C$  represents the product of mass flow rate and specific heat of blood entering the capillaries;  $H_{as}$ ,  $H_{VS}$  denote the coefficients of heat transfer between large arteries and tissue type  $s$  per unit volume and between veins and tissue type  $s$  per unit volume; and  $T_a = T_a(t)$ ,  $T_V = T_V(t)$  represent the temperatures of the blood in the arteries and veins, respectively. Numerical values for these constants are well documented in the literature and are presented concisely in [10,11,19].

(11)

It was noted earlier that the effective thermal conductivities  $k_1$ ,  $k_2$  of the core and insulating layer annuli are different. This discontinuity in conductivity means that (7) cannot be applied to points on the core/insulating layer interface. Instead a boundary condition known as *flux equality* must be used to calculate the temperature; this equation is given by

$$-\kappa_1 \frac{\partial u}{\partial r} = -\kappa_2 \frac{\partial u}{\partial r} . \quad (8)$$

When applying (7) to points at the skin surface account must be taken of the heat exchange between the skin and the environment. This exchange is governed by the derivative boundary condition

$$-\kappa_2 \frac{\partial u}{\partial r} = Q\{u - E(\theta(t))\} + S(u) , \quad (9)$$

where  $E$  is the environmental temperature and  $S$  is the heat loss due to sweating;  $Q$  depends on the microenvironment and contains terms representing heat loss due to convection, evaporation, conduction and radiation at the skin surface.

The temperature of the blood in the arteries and veins vary with time and are governed by heat balances which form a system of ordinary differential equations given by

$$\begin{aligned} (WC)_a \frac{dT_a}{dt} &= (\dot{m}C)_{ae} (T_{ae} - T_a^t) + H_{av} (T_v^t - T_a^t) \\ &+ \sum_{r=0}^a \sum_{\theta=0}^{2\pi} H_{as} (u_{r,\theta}^t - T_a^t) + q_a , \end{aligned} \quad (10)$$

$$\begin{aligned} (WC)_v \frac{dT_v}{dt} &= (\dot{m}C)_{ve} (T_{ve} - T_v^t) + H_{av} (T_a^t - T_v^t) \\ &+ \sum_{r=0}^a \sum_{\theta=0}^{2\pi} [(\dot{m}C)_{cs} + H_{vs}] (u_{r,\theta}^t - T_v^t) + q_v . \end{aligned} \quad (11)$$

In (10),(11)  $(WC)_a$  ,  $(WC)_v$  denote, respectively, the product of the specific heat and the mass of blood in the arteries and veins;  $(\dot{m}C)_{ae}$ ,  $(\dot{m}C)_{ve}$  represent the product of specific heat of blood and mass flow

(12)

rate entering the arteries and veins, respectively;  $H_{av}$  is the coefficient of heat transfer between large arteries and veins;  $T_{ae}, T_{ve}$  denote the temperature of the blood entering the arteries and veins, respectively; and  $q_a, q_v$  represent, respectively, heat loss due to respiration *via* the arterial and venous pools. The terms  $T_a^t, T_v^t, u_{r,\theta}^t$  are discretized values of  $T_a(t), T_v(t), u(r,\theta,t)$  respectively.

Equation (7) cannot be applied at the origin where  $r = 0$ . The temperature of the tissue at the origin will however be required in the numerical implementation of (7) to points surrounding the origin and its value may be taken to be the arithmetic mean of the surrounding points.

Equations (7),(10),(11) are the differential equations of the model. Initial conditions must be specified; these will vary with environmental conditions and must be determined for each numerical experiment. The boundary conditions are given by (8), (9).

In seeking a numerical solution the region occupied by the torso is discretized by a number of equally spaced points along a number of radii inclined at equal angles to each other. The equations of the model are applied to the mesh points as appropriate, approximating the space derivatives in (7),(8),(9) by finite difference replacements. This results in a system of ordinary differential equations of the form

$$\frac{d\mathbf{U}}{dt} = \mathbf{A}(\mathbf{U})\mathbf{U} + \mathbf{b}(\mathbf{U}) \quad (12)$$

where the vector  $\mathbf{U} = \mathbf{U}(t)$  is the vector of tissue temperatures at the points of discretization and blood temperatures; the sparse matrix  $\mathbf{A}$  depends on the space discretization and the physiological constants, and the elements of the vector  $\mathbf{b}$  depend on the heat source terms in (7), the physiological constants and the environmental conditions.

In [10,11,19], the non-linear equation (12) was considered to be linear in a small time interval  $\ell$  and it was thus shown that the solution of the resulting linear problem at time  $t = n\ell$  satisfies

$$\mathbf{U}(t+\ell) = \exp(\ell\mathbf{A}_n) \{ \mathbf{U}(t) + \mathbf{A}_n^{-1}\mathbf{b}_{-n} \} - \mathbf{A}_n^{-1}\mathbf{b}_{-n}, \quad (13)$$

(13)

where  $A = A_n$ ,  $\underline{b} = \underline{b}_n$  at time  $t = n\ell$ ;  $A_n$ ,  $\underline{b}_n$  are updated for each  $n = 1, 2, \dots$  (clearly  $A_0$ ,  $\underline{b}_0$  reflect the initial conditions), Replacing the exponential function in (13) by a suitable Padé approximant yields a numerical solution. In the interests of stability, the chosen Padé approximant should lead to an implicit solution and it must be capable of coping with the discontinuities between initial conditions and boundary conditions which arise following an instantaneous change in environmental temperature. In [10,11,19] the low order (1,0) Padé approximant was used and the computed results were extrapolated following Lawson and Morris [7].

## 5. SUMMARY

A number of case studies have been outlined in the present paper which show how mathematicians and medical biophysicists have collaborated to give a wider understanding of some problems in applied physiology.

For each case study, the mathematical model has been seen to lead to the numerical solution of a system of partial differential equations. One feature of the mathematical models has been the complicated boundary conditions which have arisen from the physiological aspects and geometry of the human body. The procedure to be followed in computing the numerical solution has been briefly outlined in each case, with reference to the research literature for detailed descriptions of algorithms.

## REFERENCES

1. Anliker M., Rockwell R.L. and Ogden E. (1971), "Non-linear analysis of flow pulse and shock waves in arteries"<sup>11</sup>, *ZAMP*, 22, 217-246 and 563-581.
2. Burghes D.N. and Borrie M.S. (1981), *Modelling with Differential Equations*, Ellis Horwood (distributed by Wiley in Canada).
3. Finlayson, Isla E. (1982), *Numerical Modelling of the Otolith Membrane*, B.Sc. Dissertation, Brunel University, Department of Mathematics.

4. Hudetz W.J. (1973), "A computer simulation of the otolith membrane", *Comput.Biol.Med.*, 3, 355-369.
5. Konz S., Hwang C., Dhiman B., Duncan J. and Masud A. (1977), "An experimental validation of mathematical simulation of human thermoregulation", *Comput.Biol.Med.* , 7, 71-82.
6. Kuznetz L.H. (1979), "A two-dimensional transient mathematical model of human thermoregulation", *Am.J.Physiol.*, 237 (5), R266-R277.
7. Lawson J.D. and Morris J.LI. (1978), "The extrapolation of first order methods for parabolic partial differential equations. I", *SIAM J. Numer. Anal.* , 15(6), 1212-1224.
8. Rumberger J.A. and Nerem R.M. (1977), "A method of characteristics calculation of coronary blood flow", *J. Fluid Mech.* , 82, 429-448.
9. Skalak R., Keller S.R. and Secomb T.W. (1981), "Mechanics of blood flow", *J. Biomechanical Engineering*, 103, 102-115.
10. Smith P. (1981), *Numerical Modelling of Human Thermoregulation*, Ph.D. Thesis (CNAAs).
11. Smith P. and Twizell E.H. (1982), "The extrapolation of Padé approximants in the closed loop simulation of human thermoregulation", *Appl. Math. Modelling*, 6(2), 81-91.
12. Stettler J.C., Niederer P., Anliker M. and Casty M. (1981), "Theoretical analysis of arterial hemodynamics including the influence of bifurcations", *Annals of Biomedical Engineering*, 9, 145-164 and 165-175.
13. Stolwijk J.A.J. and Hardy J.D. (1966), "Temperature regulation in man - a theoretical study", *Pflügers Archiv*, 291, 129-162.
14. Stolwijk J.A.J. and Hardy J.D. (1970), "Mathematical model of thermoregulation". In Hardy J.D. *et al* (eds.), *Physiological and Behavioral Temperature Regulation*, C.C. Thomas, Springfield, Illinois.



15. Stolwijk J.A.J. and Hardy J.D. (1977), Chapter 4 in *Handbook of Physiology (Section 9)*, American Physiological Society, Bethesda, Md.
16. Twizell E.H. (1980), "A variable gravity model of the otolith membrane", *Appl.Math.Modelling*, 4(2), 82-86.
17. Twizell E.H. (1980), "Computer simulation of arterial blood pressure with variable wave speed", *Comput.Biol.Med.*, 10(3), 123-129.
18. Twizell E.H. and Curran D.A.S. (1977), "A finite element model of the otolith membrane", *Comput.Biol.Med.*, 7, 131-141.
19. Twizell E.H. and Smith P. (1981), "Heat flow in the human torso approximated by an elliptic cylinder", Brunel University, Department of Mathematics Technical Report *TR/11/81*.
20. Wille S.φ. (1980), "Pressure and flow in arterial stenoses simulated in mathematical models", *Appl.Math.Modelling*, 4, 483-488.
21. Wille S.φ. and Wall φe L. (1981), "Pulsatile pressure and flow in arterial stenoses simulated in a mathematical model", *J.Biomed.Engng.*, 3, 17-24.

XB 2356457 1

